A ReaxFF potential for Al–ZnO systems

A ReaxFF potential for Al–ZnO systems

OPEN ACCESS
IOP Publishing
Modelling and Simulation in Materials Science and Engineering
Modelling Simul. Mater. Sci. Eng. **30** (2022) 035001 (14pp) https://doi.org/10.1088/1361-651X/ac4a25

A ReaxFF potential for Al–ZnO systems

I Brown, R Smith* and S D Kenny

School of Science and Department of Materials, Loughborough University, Leicestershire LE11 3TU, United Kingdom

E-mail: I.brown@lboro.ac.uk and r.smith@lboro.ac.uk

Received 26 August 2021, revised 9 December 2021
Accepted for publication 11 January 2022
Published 7 March 2022

Abstract

A reactive field force potential has been created in order to model the structural effects of low percentage dopant aluminium in a zinc oxide (ZnO) system. The potential's parameters were fitted to configurations computed with density functional theory: binding energies were considered for surface structures and for Al in ZnO bulk crystals. Energies for Zn–Al alloys were also considered. Forces were fit to zero for all equilibrium structures and were also fitted for some non-equilibrium structures. As a first application of the model, the energetic deposition (0.1–40 eV) of an aluminium atom onto the polar surface of a ZnO $(000\bar{1})$ is considered. For low energies the Al atom attaches to two preferred sites on the surface but as the energy increases above ≈15 eV subplantation is preferred at near normal incidence, with high diffusion barriers between stable sites. At these energies, reflection of the Al atom occurs at incident angles above ≈55°.

Keywords: ReaxFF, potential, Al–, ZnO, fitting, particle swarm

Supplementary material for this article is available online

(Some figures may appear in colour only in the online journal)

1. Introduction

Dopants of specific atoms have been have been used in thin films for many years in order to achieve specific properties. Scratch resistance, anti-glare and low-emissivity (Low-E) are all possible with specific thin films and dopants [1]. Zinc oxide (ZnO) is one such thin film coating which acts as a transparent conducting oxide for optical applications, the conductance of which has been shown to improve by the addition of small concentrations of aluminium [2].

*Author to whom any correspondence should be addressed.

Modelling the growth of multilayer thin film coatings requires good models of the interactions between atoms. *Ab initio* techniques are generally regarded as being more accurate than potential models but are computationally too slow to model deposition processes. With the advance in computational power such *ab initio* calculations can be used to fit potential models with increasing accuracy.

One such potential formulation that has proved successful in modelling thin film growth of oxides is the reactive field force (ReaxFF) formulation. For example, the growth of ZnO has been successfully modelled by Blackwell *et al* [3] using this approach. In low-E coatings Ag is used as an infra-red blocker on a ZnO lattice. The ReaxFF formulation by Lloyd *et al* were able to construct a potential and carry out growth simulations of Ag on ZnO using an adaptive kinetic Monte-Carlo method [4, 5] but so far the influence of Al on the ZnO growth process has not been considered. The aim of this work is to develop a potential that will accurately recreate low concentrations of Al interacting with the ZnO by using the existing ReaxFF model for ZnO [6] and performing *ab initio* calculations using SIESTA [7] for Al in ZnO to extend the parameterisation.

As an application of the model, the interaction of Al with the polar surface of ZnO at energies commonly found in magnetron sputtering, in the range of 0.1 to 40 eV, over a range of deposition angles [8], is considered.

2. Methodology

2.1. ReaxFF reactive force field

In order to model dynamic charge carriers accurately in complex systems, a ReaxFF model was developed. The ReaxFF potential has been used in numerous cases in order to model metals, dielectrics and the interactions between both. ReaxFF models the energy of a system by summing the individual energy contributions as shown below:

$$E_{\text{system}} = E_{\text{bond}} + E_{\text{over}} + E_{\text{under}} + E_{\text{val}} + E_{\text{pen}} + E_{\text{tors}} + E_{\text{lp}} + E_{\text{conj}} + E_{\text{vdWaals}} + E_{\text{Coulomb}} \quad (1)$$

with each term being described by the bond order of atoms i and j and the distance between them. The individual energy contributions that are dependant on the bond order are: E_{bond} which is the bond energy, E_{under} and E_{over} giving a penalty for under and over coordination terms that will make sure atoms do not exceed their total bond order, E_{val} which will take into account the valence angle terms, E_{pen} a penalty term, E_{tors} describing the torsion angles, energy contributions that are described by lone pairs E_{lp} and finally the conjugation parameters E_{conj} [9, 10].

The bond order terms have three significant contributing factors of—sigma, pi and double pi bonds:

$$\begin{aligned} \text{BO}_{ij}^{\sigma} &= \exp\left[P_{\text{bo1}}\left(\frac{r_{ij}}{r_0^{\sigma}}\right)^{P_{\text{bo2}}}\right] \\ \text{BO}_{ij}^{\pi} &= \exp\left[P_{\text{bo3}}\left(\frac{r_{ij}}{r_0^{\pi}}\right)^{P_{\text{bo4}}}\right] \\ \text{BO}_{ij}^{\pi\pi} &= \exp\left[P_{\text{bo5}}\left(\frac{r_{ij}}{r_0^{\pi\pi}}\right)^{P_{\text{bo6}}}\right] \end{aligned} . \quad (2)$$

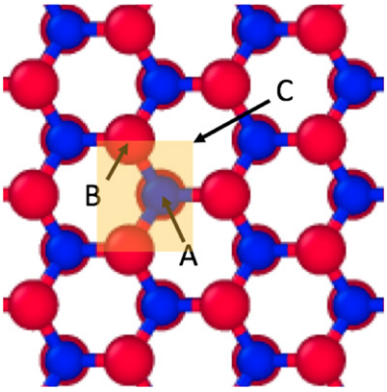

Figure 1. The possible adsorption sites for an Al atom on the polar surface of ZnO. The O atoms are coloured red and the Zn blue. The shaded region is the irreducible symmetry zone of the surface.

Table 1. Table to show the relative weights applied on each system during the fit.

System type	Weight
Alloy FCC (eV)	0.50
Alloy HCP (eV)	0.50
Interstitial wurtzite (eV)	0.60
Single substitution wurtzite (eV)	0.70
Double substitution wurtzite (eV)	0.70
Triple substitution wurtzite (eV)	0.70
Single substitution zincblende (eV)	0.60
Double substitution zincblende (eV)	0.60
Single surface wurtzite (eV)	1.00
Double surface wurtzite (eV)	0.90
Triple surface wurtzite (eV)	0.90
Forces (Kcal mole^{-1} Angstrom^{-1})	0.005

In order to consider the full bond order term, each contribution needs to be summed together as shown by:

$$\mathrm{BO}_{ij} = \mathrm{BO}_{ij}^{\sigma} + \mathrm{BO}_{ij}^{\pi} + \mathrm{BO}_{ij}^{\pi\pi}. \tag{3}$$

The terms of E_{vdWaals} and E_{Coulomb} are not dependent on the bond order. In previous fits of ReaxFF it has been seen that some of these terms can be removed as not all of the terms are essential for a good fit.

$$E_{\mathrm{system}} = E_{\mathrm{bond}} + E_{\mathrm{over}} + E_{\mathrm{under}} + E_{\mathrm{val}} + E_{\mathrm{lp}} + E_{\mathrm{vdWaals}} + E_{\mathrm{Coulomb}}. \tag{4}$$

2.2. Computational details

Density functional theory (DFT) calculations were performed using the SIESTA package in order to provide quantum-chemical calculations with the same functionals and pseudopotentials as used in [5].

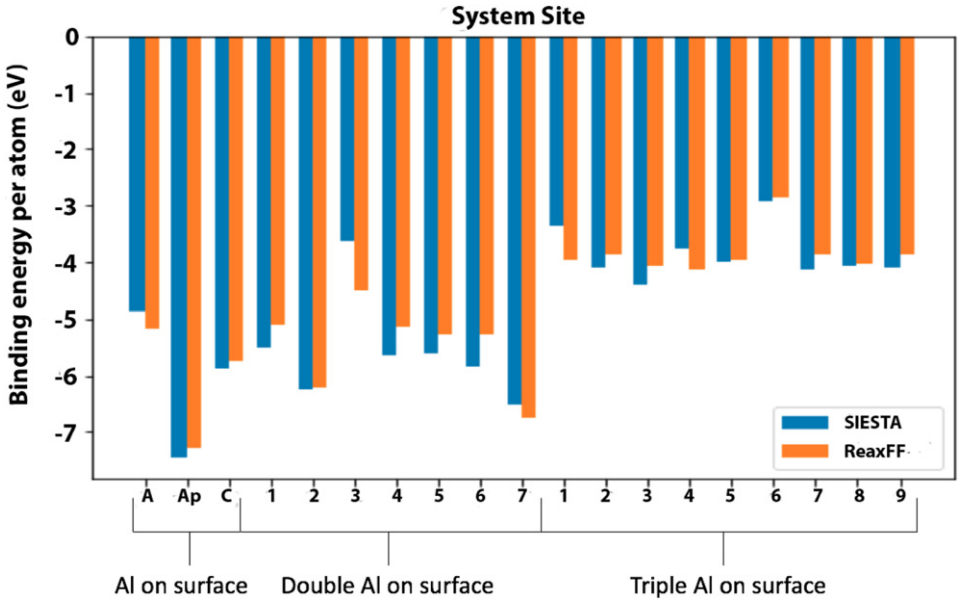

Figure 2. A comparison between energies of single, double and triple aluminium on the polar ZnO wurtzite surface.

Table 2. Table to show the relative binding energies of each site on the surface between SIESTA and ReaxFF.

Site	E_{Siesta} (eV)	E_{ReaxFF}(eV)
A	−4.89	−5.16
A_p	−7.46	−7.27
C	−5.87	−5.73
C_p	−6.20	−6.07

The systems chosen for the fitting process were the Al–Zn alloy in face centred cubic (FCC) and hexagonal closed packed (HCP) form, Al and double Al interstitials in ZnO, Al substitutional structures in ZnO and Al on a ZnO surface. The cohesive energies of the alloys and the binding energies of Al on the wurtzite surface of ZnO were calculated in SIESTA and compared to the ReaxFF model. For substitutional Al in the bulk lattices, the lattices were expanded so that non-equilibrium structures were also fitted. For the surfaces, some non-equilibrium structures were also considered and the forces as well as the binding energies used in the fitting process.

It was intended that the main application for the fitted potential would be to understand the structural implications of small amounts (approximately 97% Zn to 3% Al) of Al in ZnO during crystal growth of transparent conducting oxides since small percentages improve electrical conductance. Thus these systems were selected to give a good description of the numerous likely cases that will occur during the growth of small amounts of Al in ZnO. The FCC and HCP systems model direct interactions between the Al and Zn atoms. These systems will not give a good model of the three body terms in the potential. The bulk and surface ZnO systems will more heavily influence these parameters.

Table 3. The transition barriers for Al diffusion on the surface of ZnO, determined by the nudged elastic band method from ReaxFF.

Initial	Final	E_B (eV)
A	C	1.35
C	A	2.08
C	A_p	1.77
A_p	C	4.25
A	A_p	1.74
A_p	A	4.95
C_p	C	4.10
C	C_p	2.51
A_P	C_p	3.22
C_P	A_p	2.34

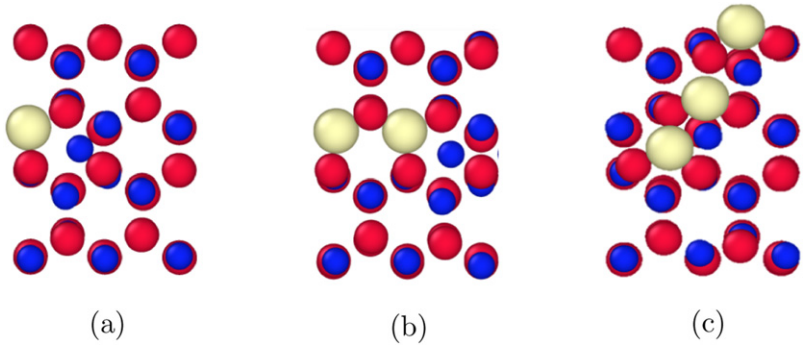

Figure 3. Examples of the most stable Al sites on the surface of ZnO wurtzite; (a) single Al in the A_p site with the displaced Zn atom on the surface; (b) double Al on the surface; (c) triple Al on the surface.

The surface systems were selected by placing Al onto the stable surface sites predicted by SIESTA. The sites are shown in figure 1. Sub-surface atom positions are also considered together with single, double and triple Al on the surface.

In all cases the forces for the equilibrium positions were fitted to zero and forces were also fitted in the case of a single Al atom approaching normally its most favoured binding position on the wurtzite surface.

The binding energy of Al ad-atoms on the surface is defined by:

$$E_{\text{bind}} = \left[E_{\text{Al/ZnO}} - E^{\text{ZnO}}_{\text{slab}} - n \cdot E^{\text{Al}}_{\text{bulk}}\right]/n, \tag{5}$$

where $E_{\text{Al/ZnO}}$ is the energy of the full system, $E^{\text{ZnO}}_{\text{slab}}$ is the energy of a clean ZnO wurtzite slab and $E^{\text{Al}}_{\text{bulk}}$ is the energy of the of Al in a bulk lattice.

In order to minimise the error between the calculations done in SIESTA and ReaxFF an error term can be defined by:

$$Err = \sum_{i=1}^{n} \left[\omega^i \sqrt{(x^i_{\text{dft}} - x^i_{\text{ReaxFF}})^2}\right], \tag{6}$$

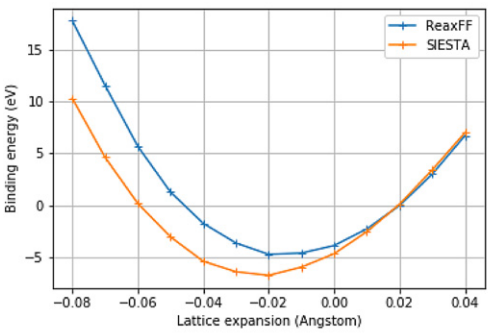

(a) Substitutional Al in expanded wurtzite

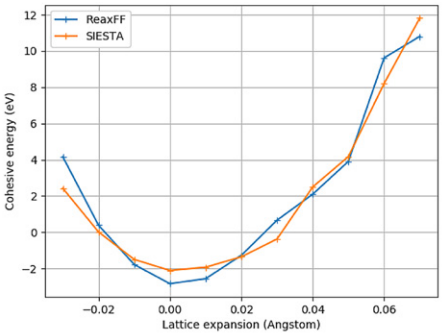

(b) Interstitial Al in expanded wurtzite

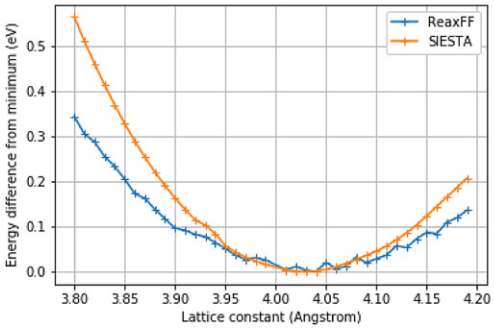

(c) The energy increase in the Zn_2Al_2 fcc alloy under uniform expansion.

Figure 4. Comparison of the differences in binding energy between SIESTA and ReaxFF for interstitial (a) and substitutional (b) Al in wurtzite. The energy differences between the FCC Zn_2Al_2 alloy under uniform lattice expansion and contraction are shown in (c).

where ω^i is used as a weight. x^i_{dft} is the energy/force of the DFT system and x^i_{ReaxFF}) is the corresponding ReaxFF value. The parameters to be fit must be carefully chosen so as to be consistent with existing ReaxFF parameterisation for Zn:O and Al:O. Thus in the fitting process only the parameters corresponding to systems, where Al and Zn were present together, were considered.

ReaxFF parameters can be separated out into several different sub-parameters of: bond parameters, off diagonal terms and angular terms. A total of 92 parameters needed to be fit. These parameters are highlighted in the input files for the application of ReaxFF in molecular dynamics (MD) codes in the supplementary data, available online at https://stacks.iop.org/MSMS/30/035001/mmedia.

2.3. Error optimisation

The particle swarm optimisation (PSO) distributes a large number of 'particles' across the parameter space as the search occurs [11]. Depending on how good the specific parameterisation is, the particle will create a force which will act on all other particles drawing them in closer. This will cause the system to evolve and continue to improve on the swarm's current best solution. PSO also allows us to specify how many 'particles' are used in the search and at

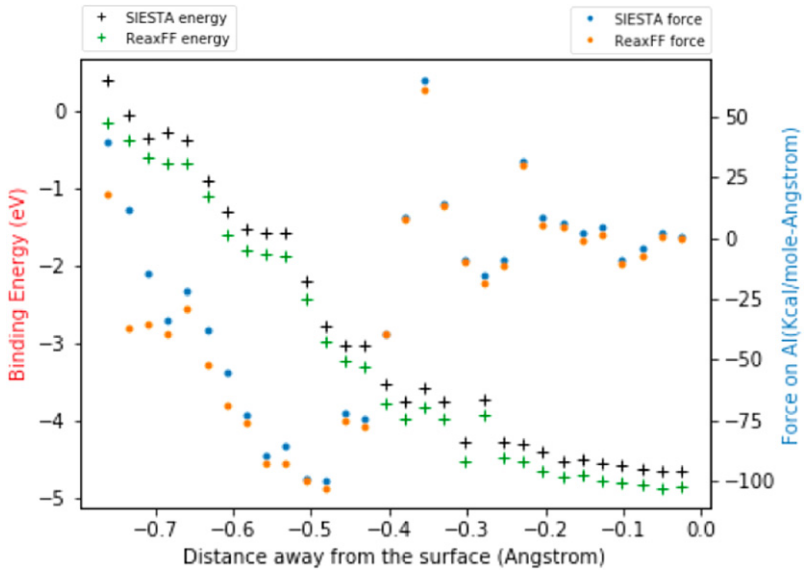

Figure 5. A comparison between ReaxFF and SIESTA for the binding energy and force on a single Al as a function of distance from a wurzite ZnO surface.

each step the algorithm will be able to specify both the position and velocity of the i'th particle in a set of n particles at step m can be evaluated using:

$$x_i^m = x_i^{m-1} + v_i^m \tag{7}$$

and

$$v_i^m = \omega v_i^{m-1} + c_1 r_1^m (x_B - x_i^{m-1}) + c_2 r_2^m (x_G - x_i^{m-1}), \tag{8}$$

where ω, $c1$ and $c2$ are hyper-parameters of the particle swarm which are commonly set to: $\omega = 0.9$, $c1 = 0.5$ and $c2 = 0.3$. These parameters are the default values specified in the PSO package in Python. Changes to this will only effect the time taken to optimise to the minimum and how each particle will interact when considering the force interactions with other atoms. Methods of selecting the parameters have been studied in depth, see for example [12].

We can define how good each of the particles' fit is, based on the objective function that we defined in equation (5). A main benefit of the PSO is that it allows a global search of the parameters without knowing anything about the parameter space. Minimisation is also performed without evaluating the differential of the objective function. It will also be able to locate minima throughout the parameter space and be able to compare all of them against each other to find the best fit. This method of optimisation has been used in the past to fit multiple different kinds of potential such as Lennard-Jones, embedded atom method [13] and ReaxFF [14].

2.4. Weights

In order to model a good potential for Al:ZnO, weights for each system need to be decided upon based on how important each system is to problem that we want to use the potential for. The focus here is the interaction of small numbers of Al atoms with surface of ZnO and their transitory states to a bulk like lattice. The most stable form of ZnO is wurtzite but zincblende

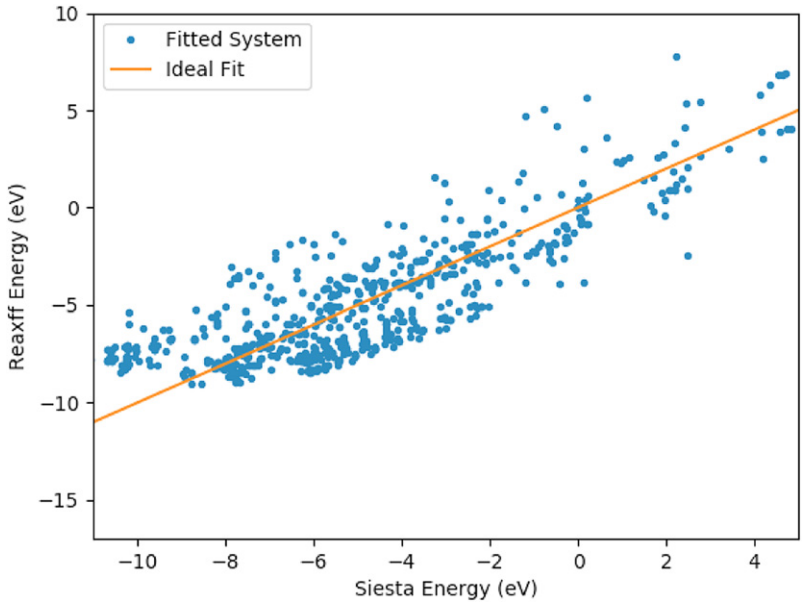

Figure 6. A comparison between the SIESTA values for the energies of the fitted structures and the ReaxFF data.

is also a stable structure of ZnO [15, 16]. As wurtzite is more likely, Al in these systems were weighted higher than in zincblende. Surface systems and bulk structures of ZnO:Al were also weighted higher than the purely metallic Zn–Al alloys which were also modelled. For the final fit of ZnOAl the weights chosen for each system were as follows:

The difference in weights seen in table 1 were manually optimised via use of multiple runs of the fitting process. A main objective of the fitting was to develop a potential that could be used to model the growth of Al doped ZnO. Thus the weights were adjusted so that configurations that were likely to arise in a growth process were accurately modelled. This is the reason why surface sites were given a higher weighting compared to the systems of Zincblende and alloys of ZnAl.

The reason that low weights were used for the forces is only because of the difference in units. In LAMMPS, forces are given in kcal mole^{-1} Å^{-1} as shown in figure 5 and these have much larger numerical values than the binding energies given in eV. The ReaxFF forces on Al atoms in equilibrium structures predicted by SIESTA were fitted to zero so that sites that were predicted by SIESTA matched those predicted by the potential.

As seen in table 1 the weights applied on each system vary between 0.5 for the less important systems to 1.0 for the more important system.

The final set of fitted parameters are given in the supplementary data, highlighted in red as they would appear in a normal ReaxFF input file.

3. Results and discussion

3.1. Binding energies

The three stable adsorption sites for Al on the ZnO wurtzite surface are shown in figure 2. Al shows a preference of sitting on either the above-hole site (C), the site below C_p or replacing the Zn in the first layer of ZnO lattice (A_p); this is likely as Al interacts with O by forming

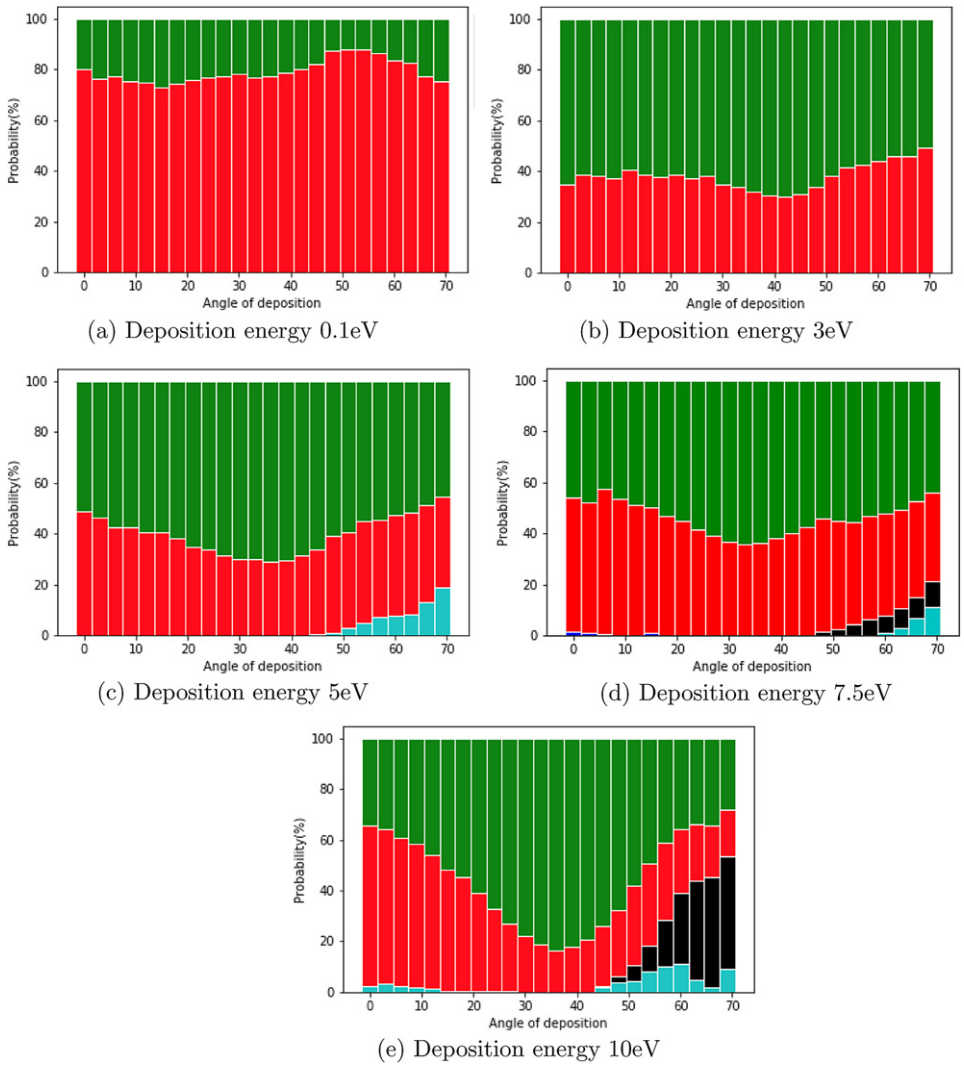

Figure 7. Relative probability, as a function of polar angle, for Al penetration into the A_p site and push Zn to surface (cyan), adsorption to C site (red), adsorption to A site (green), reflection (black).

Al_2O_3 [17]. The relative binding energies are shown in table 2, showing reasonable agreement between SIESTA and ReaxFF. For this data, the A, A_p and C sites were used in the fitting data but the C_p site was not fitted explicitly so could be regarded as testing data for the model.

As shown in table 2 there are two likely sites on the surface at A, one of which labelled A in the table is the Al sitting on the A site in the surface as defined in figure 1. A_p is when the Al penetrates into the A site and shifts a Zn atom onto the surface. C_p represents penetration of the Al atom to an interstitial position below the surface at the C site. The A_p site is the most stable but the relatively high energy barriers between the various sites as given in table 3 show that Al

is likely to remain stably bonded to the other sites after deposition at low temperature. These barriers were determined by using the nudged elastic band method in the ReaxFF model.

The surface structures for double and triple Al show also good agreement between SIESTA and the ReaxFF data as shown by in figure 2 with some corresponding structures in figure 3.

Figure 4 shows how the energy of Al changes in bulk structures under uniform expansion. The ReaxFF parameters were also fitted to the SIESTA data for these systems.

The energy differences between the equilibrium structure and that of the expanded FCC and HCP Zn–Al alloys were fitted over 4.5% lattice expansion and contraction. Figure 4(c) gives a lattice constant of ≈4.02 Å for the FCC alloy for both ReaxFF and SIESTA but the curvatures at the equilibrium spacing and therefore elastic properties do not match exactly. This is partially due to this system not having a high weighting during the fit as surface structures were regarded as more important.

The other non-equilibrium structures that were considered in the fitting were the positions of the single, double and triple Al clusters close to the surface. Initially these were placed above the surface and conjugate gradient minimisation used in SIESTA to determine the final structure. During minimisation the clusters approach the surface. The forces on the Al atoms were determined and these also used together with the binding energy to fit the ReaxFF model. The example for single Al atom is shown in figure 5. In total together with the energy calculations 1320 separate data points were fitted.

Figure 6 illustrates the goodness of fit for the cases where energies were fitted. Reasonable agreement can be seen across a range of energies. Analysis of the data shows that 80% of all systems are within 2 eV of a perfect fit.

4. Application

The ultimate aim of the work was to model the growth of Al-doped ZnO by magnetron sputtering. In this process energetic atoms, mostly in the energy range 0–40 eV but over a range of deposition angles are incident on the surface [19]. To understand the mechanisms by which Al atoms in this energy range attach to the surface, a series of individual trajectory calculations using classical MD were carried out for a single Al atom incident on ZnO over a wide range of energies and incidence angles at 300 K.

The outcome of the Al interactions with the surface will depend on the point of the surface towards which the Al atom is projected. The smallest area on a surface which when repeated can describe the entirety of the surface is known as the irreducible symmetry zone. This zone for ZnO wurtzite is shown in figure 1. This region was divided into a 20×20 equally spaced grid and Al atoms projected towards points on this grid.

A grid of angles also needs to be considered to generate good statistics. The polar angle θ was chosen to vary from 0–69° in 3° steps. For $\theta = 0°$, only 1 azimuthal angle was chosen, for $\theta = 3°$, 2, for $\theta = 6°$, 3 up to $\theta = 42°$ and above when 15 were chosen. ZnO wurtzite has six fold symmetry [18] so the azimuth angle was varied from 0–60°. These points were then uniformly spaced using the Thomson method [20]. For each energy the total number of trajectory calculations was 42 400.

4.1. Single Al deposition results

In figure 7 it can be seen that when Al is deposited on the surface at energies ranging between 0.1 and 5 eV (normal to the surface) there is no penetration. As the deposition energy passes

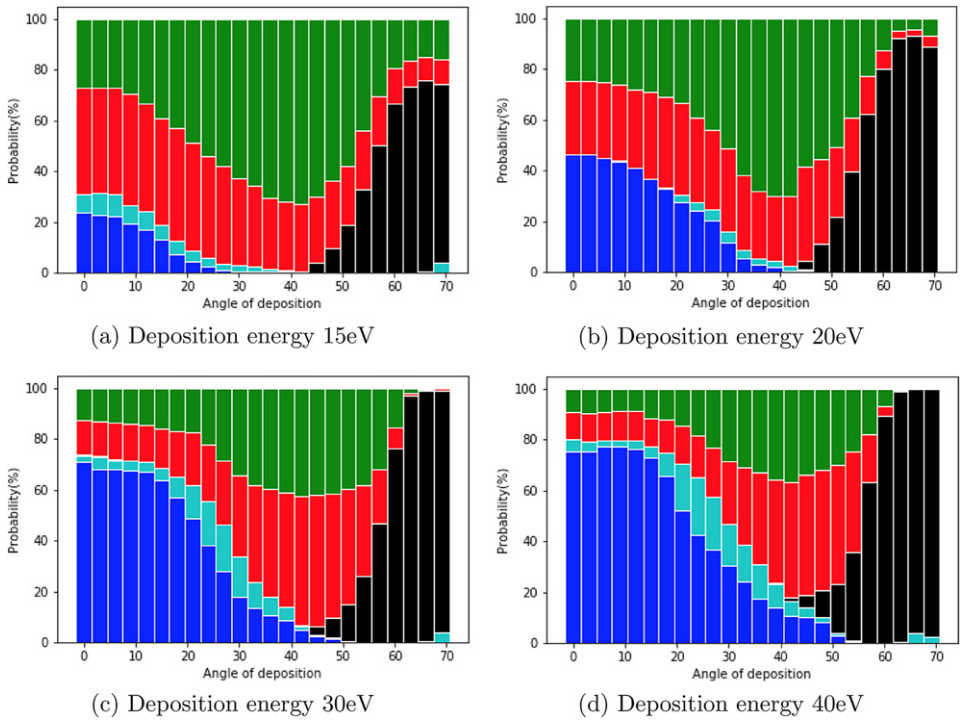

Figure 8. Relative probability, as a function of polar angle, for Al penetrating into the C_p site (blue), penetrating into the A_p site and push Zn to surface (cyan), adsorption to C site (red), adsorption to the A site (green), reflection (black).

$\approx$ 5 eV, the likelihood of penetration begins to increase. On the surface itself the C site is more stable than the A site, so at very low energies there is a higher probability of adsorption at this site. This changes as the energy increases to 3 eV with the A site being more favoured as now the Al atom has enough energy to continue on its trajectory and overcome the attraction to the C site. At around 5 eV and incidence angles of 50° and more there is enough energy imparted for the Al to knock out a Zn atom and access the A_p site. At 10 eV the A_p site can be accessed by both normally and obliquely incident atoms and reflection can also occur.

At 15 eV as shown in figure 8 the C_p site begins to be accessed. Once the Al atom is implanted at the A_p and C_p sites table 2 shows that the energy barriers to escape are very high. At energies of 20 eV and more the C_p site becomes the most favoured with a large number of reflected Al at angles of 60° and more. As expected, as the energy of the incoming atom increases more and more Al atoms subplant so that at 40 eV nearly 80% of all impacts reach the C_p site for incident angles up to $\approx$15°.

Finally figure 9 gives a plan view of the surface A and C sites where the incident atoms are located after deposition. It can be seen that even at an incident energy of 10 eV the Al atom can attach to the surface several Å distant from the point to which it was originally projected.

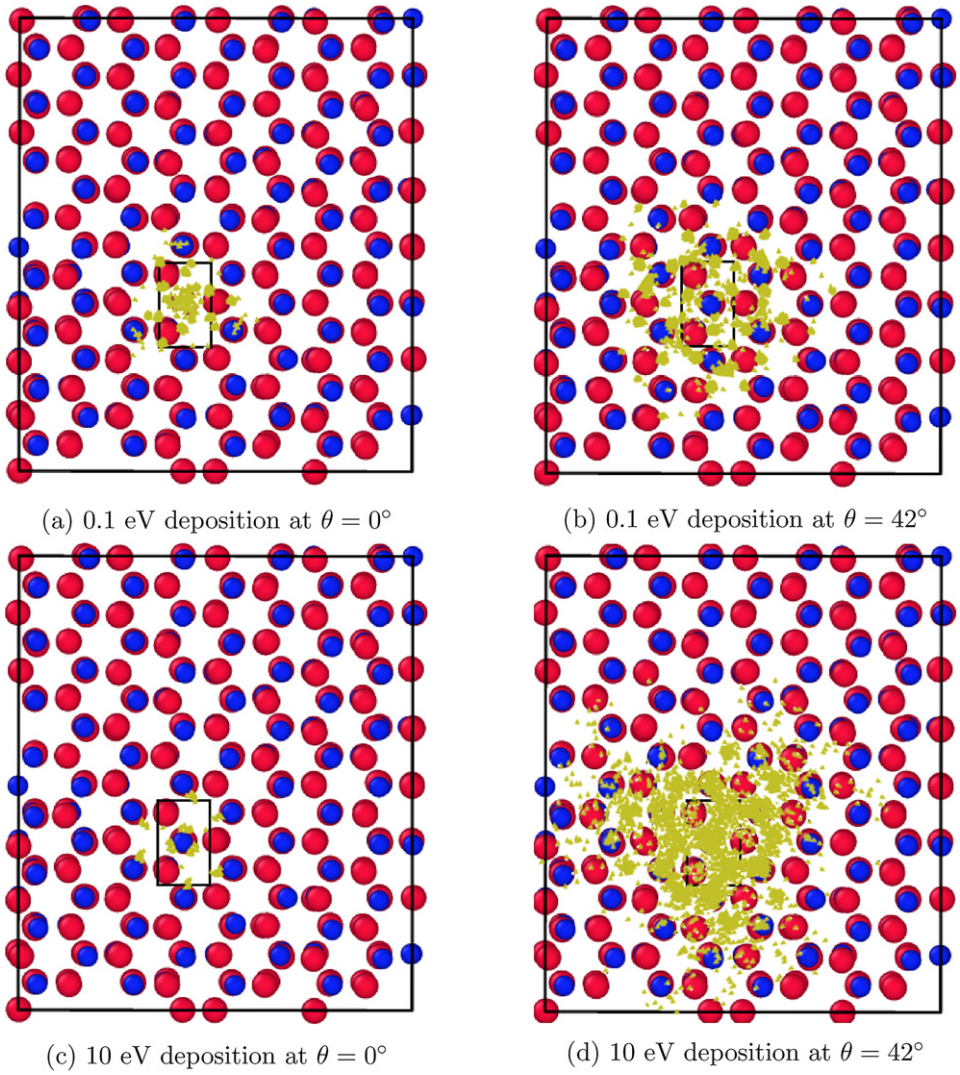

Figure 9. Final adsorption sites of Al on a ZnO wurtzite surface. The yellow dots indicate the sites and the black rectangle the irreducible symmetry zone to which the Al atoms are projected.

5. Conclusion

A ReaxFF potential for small percentages of Al in ZnO has been developed consistent with previous parameterisations of ZnO. The potential has not been fitted for large concentrations of Al where a spinel structure might be expected, but should be applicable for describing structural properties of ZnO with low concentrations of Al. The *ab initio* code SIESTA was used in the fitting process with generally good agreement for surface structures. The Zn–Al alloy structures were also used in the fitting process with good agreement near equilibrium.

The model shows that it is energetically preferable for an Al atom to be subplanted below the surface of ZnO but there is an energy barrier to be overcome for this to happen and this site

is never accessed for impact energies of 10 eV or less. The energy barriers to diffuse are large so that in a co-deposition process Al is unlikely to aggregate into small clusters.

Individual trajectory calculations using MD give confidence that the potential can be used for longer time growth simulations as for example for ZnO [21] so that structures occurring in thin film growth of Al doped ZnO can be analysed and optimised.

Archived data

All data that has been used in the ZnOAl fit can be found in the Loughborough University Repository at:

Surface zincblende data: https://doi.org/10.17028/rd.lboro.16912645
Surface wurtzite systems: https://doi.org/10.17028/rd.lboro.16912633
Zincblende larger: https://doi.org/10.17028/rd.lboro.16912552
Zincblende smaller: https://doi.org/10.17028/rd.lboro.16912525
Wurtzite SIESTA data: https://doi.org/10.17028/rd.lboro.16912477

Acknowledgments

We acknowledge partial funding from Asahi Glass Europe. Thanks are also given to HPC midlands for high performance computer time.

Data availability statement

All data that support the findings of this study are included within the article (and any supplementary files).

ORCID iDs

I Brown https://orcid.org/0000-0003-2890-3482
R Smith https://orcid.org/0000-0001-8147-431X
S D Kenny https://orcid.org/0000-0003-3285-2403

References

[1] Šimurka L, Čtvrtlík R, Tomaštík J, Bektaş G, Svoboda J and Bange K 2018 Mechanical and optical properties of SiO_2 thin films deposited on glass *Chem. Pap.* **72** 2143–51
[2] Nunes P, Fortunato E, Tonello P, Braz Fernandes F, Vilarinho P and Martins R 2002 Effect of different dopant elements on the properties of ZnO thin films *Vacuum* **64** 281–5
[3] Blackwell S, Smith R, Kenny S, Walls J and Sanz-Navarro C 2013 Modelling the growth of ZnO thin films by PVD methods and the effects of post-annealing *J. Phys.: Condens. Matter.* **25** 135002
[4] Lloyd A, Cornil D, van Duin A C T, van Duin D, Smith R, Kenny S D, Cornil J and Beljonne D 2016 Development of a Reaxff potential for Ag/Zn/O and application to Ag deposition on ZnO *Surf. Sci.* **645** 67–73
[5] Lloyd A L, Smith R and Kenny S D 2017 Critical island size for Ag thin film growth on ZnO (0 0 0$\bar{1}$) *Nucl. Instrum. Methods Phys. Res.* B **393** 22–5
[6] Raymand D, van Duin A C T, Baudin M and Hermansson K 2008 A reactive force field (ReaxFF) for zinc oxide *Surf. Sci.* **602** 1020–31

[7] Soler J *et al* 2002 The SIESTA method for *ab initio* order-*N* materials simulation *J. Phys.: Condens. Matter.* **14** 2745–79
[8] Oh B-Y, Jeong M-C, Lee W and Myoung J-M 2005 Properties of transparent conductive ZnO:Al films prepared by co-sputtering *J. Cryst. Growth* **274** 453–7
[9] Raymand D, van Duin A C T, Spångberg D, Goddard W A and Hermansson K 2010 Water adsorption on stepped ZnO surfaces from MD simulation *Surf. Sci.* **604** 741–52
[10] van Duin A C T, Dasgupta S, Lorant F and Goddard W A 2001 Reaxff: a reactive force field for hydrocarbons *J. Phys. Chem* A **105** 9396–409
[11] Iwamatsu M 2006 Locating all the global minima using multi-species particle swarm optimizer: the inertia weight and the constriction factor variants *Int. Conf. on Evolutionary Computation* pp 816–22
[12] Haidar A, Field M, Sykes J, Carolan M and Holloway L 2021 PSPSO: a package for parameters selection using particle swarm optimization *SoftwareX* **15** 100706
[13] González D and Davis S 2014 Fitting of interatomic potentials without forces: a parallel particle swarm optimization algorithm *Comput. Phys. Commun.* **185** 3090–3
[14] Furman D, Carmeli B, Zeiri Y and Kosloff R 2018 Enhanced particle swarm optimization algorithm: efficient training of ReaxFF reactive force fields *J. Chem. Theory Comput.* **14** 3100–12
[15] Meyer B and Marx D 2003 Density-functional study of the structure and stability of ZnO surfaces *Phys. Rev.* B **67** 035403
[16] Ashrafi A and Jagadish C 2007 Review of zincblende ZnO: stability of metastable ZnO phases *J. Appl. Phys.* **102** 071101
[17] Jeurgens L P H, Sloof W G, Tichelaar F D and Mittemeijer E J 2002 Structure and morphology of aluminium-oxide films formed by thermal oxidation of aluminium *Thin Solid Films* **418** 89–101
[18] Casella R C 1959 Symmetry of wurtzite *Phys. Rev.* **114** 1514–8
[19] Ellmer K 2000 Magnetron sputtering of transparent conductive zinc oxide: relation between the sputtering parameters and the electronic properties *J. Appl. Phys.* **33** R17–32
[20] Batle J, Bagdasaryan A, Abdel-Aty M and Abdalla S 2016 Generalized Thomson problem in arbitrary dimensions and non-Euclidean geometries *Physica* A **451** 237–50
[21] Blackwell S 2012 Modelling thin film growth over realistic time scales *PhD Thesis* (Loughborough University, Sabrina Blackwell)